J Fluoresc (2008) 18:119–129
DOI 10.1007/s10895-007-0250-9

ORIGINAL PAPER

Improving Visible Light Sensitization of Luminescent Europium Complexes

Pascal Kadjane · Loïc Charbonnière · Franck Camerel · Philippe P. Lainé · Raymond Ziessel

Received: 21 March 2007 / Accepted: 4 September 2007 / Published online: 2 October 2007

Abstract The synthesis and characterization of the new ligands $\mathbf{L_1}$, $\mathbf{L_2}$ and $\mathbf{L_4}$ are described with the series of four europium complexes of formula [Eu$\mathbf{L_n}$(TTA)$_3$] in which TTA refers to 2-thenoyltrifluoroacetonate and $\mathbf{L_n}$ to tridentate ligands with nitrogen containing heterocyclic structure, such as a 2,6-bis(3-methyl-pyrazolyl)-4-(*p*-toluyl-ethynyl)-triazine for $\mathbf{L_1}$, or terpyridines functionalized at the 4′ position by a phenyl-vinylene for $\mathbf{L_2}$, a *p*-dimethylamino-phenylene for $\mathbf{L_3}$, or a *p*-aminophenyl-ethynylene for $\mathbf{L_4}$. The spectroscopic properties of the ligands and of the complexes are studied by means of UV–Vis absorption spectroscopy, as well as steady-state and time-resolved luminescence spectroscopy. All complexes display europium centred luminescence upon ligand excitation. Careful examination of the excitation spectra revealed differences in the ligand based sensitization efficiencies. For complexes of $\mathbf{L_1}$ and $\mathbf{L_2}$, excitation of europium is mainly achieved through the TTA moieties and the photo-physical studies on [Eu$\mathbf{L_1}$(TTA)$_3$] evidenced a weaker coordination of the bispyrazolyltriazine tridentate ligand, resulting from a partial decomplexation upon dilution. Complexes of $\mathbf{L_3}$ and $\mathbf{L_4}$ display intense excitation through the tridentate units, which extend down to 460 nm in the visible region. In the case of $\mathbf{L_3}$, selective excitation reveals the presence of a ligand-centred emission band at 520 nm which is likely ascribed to a $\mathbf{L_3}$ centred charge transfer state.

Keywords Europium complexes · Sensitization efficiency · Visible excitation · Terpyridine ligands · Charge transfer state

P. Kadjane · L. Charbonnière (✉) · F. Camerel · R. Ziessel
Laboratoire de Chimie Moléculaire,
CNRS UMR 7509, ECPM–ULP,
25 rue Becquerel,
67087 Strasbourg Cedex, France
e-mail: charbonn@chimie.u-strasbg.fr

P. P. Lainé
Laboratoire de Chimie et Biochimie Pharmacologiques et Toxicologiques, CNRS UMR-8601, Université René Descartes,
45 rue des Saints Pères,
75270 Paris Cedex 06, France

Introduction

The peculiar photophysical properties of luminescent lanthanide complexes trigger numerous research efforts. In particular, their long lived luminescent excited states together with narrow emission bands are of interest for various analytical applications [1]. Among others, lanthanide complexes have found outlets as luminescent labels and markers [2, 3], as lasing materials or as active components in electroluminescent devices [4]. Due to the strongly forbidden character of *f–f* transitions, direct excitation of lanthanide ions is hardly obtained through direct means without laser sources. To circumvent this drawback, it has been found that excitation of chromophoric units introduced in the first coordination sphere of lanthanide cations or in its close vicinity can result in energy transfer from the chromophore to the lanthanide. This process, often called antenna effect [5], has been early demonstrated by Weissmann for excitation of Eu with ligands absorbing in the UV region [6], and was subsequently extended to sensitization of numerous luminescent complexes emitting in the visible domain for Eu, Tb, Sm, Ho and Dy, or in the near infrared domain with Ho, Tm, Pr, Nd, Yb and Er [7, 8]. Different mechanisms for the process governing ligand-based photosensitization have been proposed in the literature. The most commonly admitted is that of a ligand singlet state absorption, followed by an Inter System Crossing (ISC) to the triplet state, which transfers

energy to form the lanthanide excited state [9]. This mechanism was substantiated by the systematic study of singlet and triplet energy levels in numerous lanthanide complexes of Eu and Tb, which demonstrated a relationship between sensitization efficiency and ligand based energy levels [9, 10]. It nonetheless remains that in some special cases sensitization can not be explained by the former mechanism. Examples mostly concern ligands with a high degree of charge transfer character in their excited states. Typical cases are encountered with Michler's ketones (4,4′-dimethylamino benzophenone, upper left ligand in the Chart) [11] containing both an electron withdrawing carbonyl moiety and electron donating aromatic amines. More recently the possibility of direct excitation by the singlet state was revisited with a ligand based on dimethylaminophenyl triazine substituted with two methylpyrazol rings, $\mathbf{L_0}$ (chart) [12]. The coordination of $\mathbf{L_0}$ to europium combined to three bidentate thenoyltrifluoroacetonate (TTA) was shown to lead to highly luminescent complexes that can be excited in the visible domain. Based on kinetic parameters for depopulation of the singlet state, it was postulated that sensitization occurs in that case directly through the singlet excited state of the ligand. In fact, in most of these complexes, the energy gap between singlet and triplet states is small and an intermediate ISC process is difficult to evidence. Whether the excitation occurs directly from the singlet state or through a closely lying triplet state remains unclear. Finally, it is worth noting that in the case of electroactive Ln(III) cations such as Eu and Yb, redox processes can also be postulated for some photosensitization processes [13].

In an attempt to get insights into the excitation mechanism and to engineer novel ligands absorbing in the visible part of the electromagnetic spectrum, we designed a series of ligands based on neutral tridentate heteroaromatic coordinating units that, in combination with three bidentate TTA anions, fulfill the first coordination sphere of the Eu cation. The ligands $\mathbf{L_1}$ to $\mathbf{L_4}$ (chart) display similar coordinating domains, but differ by the nature of their substituents playing a role in both the delocalization and the polarization of the electronic clouds.

Ligand $\mathbf{L_1}$ was taken as an equivalent of $\mathbf{L_0}$ lacking the diethyl amine electron donating moiety, replaced by a weakly electron withdrawing group. The effect of changing the N3 tridentate coordination from a bis-pyrazolyltriazine to a terpyridine can then be derived from comparison with ligand $\mathbf{L_2}$, also deprived of electron donating groups. Next, keeping the tridentate terpyridine core, the contribution of electron donating functions was studied by comparing the photophysical behavior of ligands $\mathbf{L_1}$ and $\mathbf{L_2}$ to those of $\mathbf{L_3}$ and $\mathbf{L_4}$. Finally, the introduction of an ethynyl spacer between the central pyridine ring of the terpyridine and the amino-functionalized phenyl rings would give an insight into the study of the possible influence of extended electronic delocalization on the photophysical properties.

Results and discussion

Synthesis of the ligands Synthetic routes for ligands $\mathbf{L_1}$, $\mathbf{L_2}$ and $\mathbf{L_4}$ are described in Scheme 1. Ligand $\mathbf{L_3}$ was synthe-

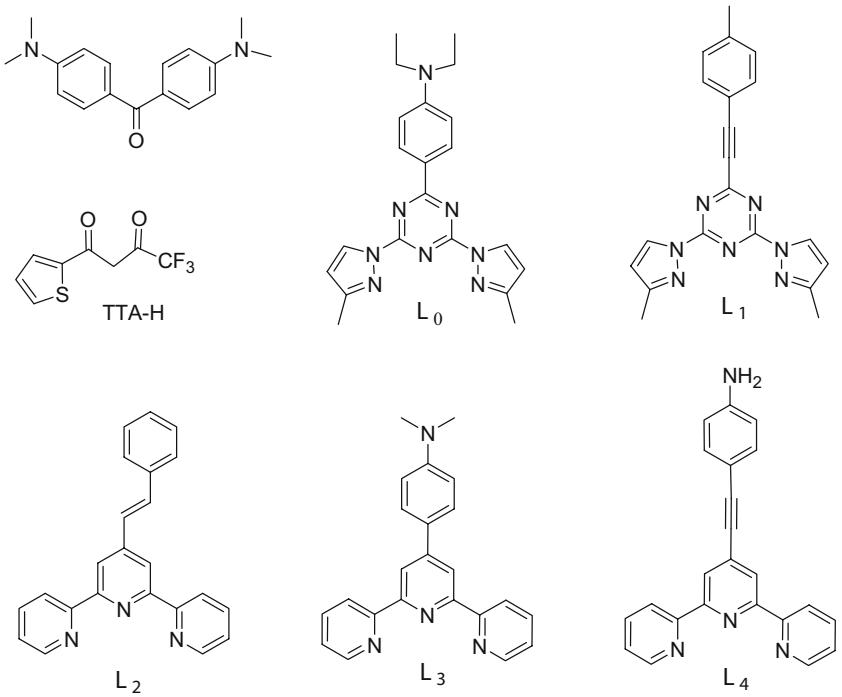

Scheme 1 Synthetic routes for ligands $\mathbf{L_1}$, $\mathbf{L_2}$ and $\mathbf{L_4}$

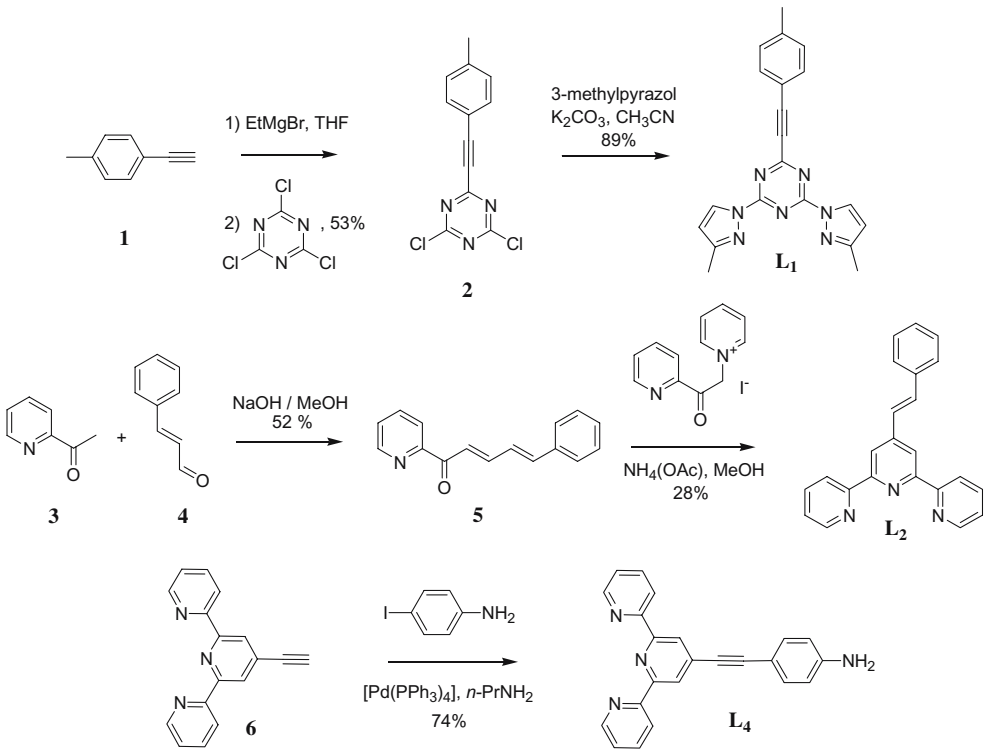

sized according to literature procedure [14]. $\mathbf{L_1}$ was obtained in three steps by first reacting magnesium ethylbromide with *p*-tolyl-acetylide **1**, which was allowed to react in situ with trichlorocyanuric acid to give compound **2**. Reaction of 3-methyl-pyrazol with **2** afforded $\mathbf{L_1}$ in 89% yield. Ligand $\mathbf{L_2}$ was obtained in two steps according to Scheme 1.

Reaction of cinnamaldehyde **4** with one equivalent acetylpyridine **3** in basic methanol first gave the azachalcone **5**, which is condensed with the pyridinium salt of acetylpyridine in the presence of ammonium acetate in a Kröhnke type protocol [15] to generate the terpyridine core of $\mathbf{L_2}$ in 14% overall yield. Finally, ligand $\mathbf{L_4}$, was obtained through a Pd(0) coupling reaction of the 4′-ethynyl-2,2′:6′,6″-terpyridine **6** [14] with 4-iodoaniline in 74% yield. All new ligands and intermediates were unambiguously characterized by ^{1}H- and ^{13}C–NMR, mass spectrometry, infrared spectroscopy and elemental analysis.

Synthesis and characterization of the complexes The europium complexes of general formula [Eu$\mathbf{L_n}$(TTA)$_3$] (n=1 to 4) were synthesized using an unified protocol, by condensation of [Eu(TTA)$_3$(H$_2$O)$_2$] in situ prepared in methanol with one equivalent of the corresponding ligand $\mathbf{L_n}$ dissolved in dichloromethane. All [Eu$\mathbf{L_n}$(TTA)$_3$] complexes were characterized by means of infrared spectroscopy, elemental analysis and mass spectrometry to ascertain the proposed formula.

Photophysical properties of the ligands and complexes Table 1 summarizes the main electronic and photophysical properties of ligands $\mathbf{L_1}$ to $\mathbf{L_4}$ obtained in air equilibrated CH_2Cl_2,

Table 1 Photophysical properties of $\mathbf{L_1}$ to $\mathbf{L_4}$ in air equilibrated CH_2Cl_2 solutions at room temperature

	Absorption	Emission				
	λ_{max}/nm (ε/M^{-1} cm^{-1})	$\lambda_{fl.}$ (nm), E (cm^{-1})	τ_{fl} (ns)	Φ_{fl} (%)	k_r[a] (×10^9 s^{-1})	k_{nr}[b] (×10^9 s^{-1})
$\mathbf{L_1}$	308 (36,100) 277 (48,500)	410 (24,400)	2.2	5	0.45	8.64
$\mathbf{L_2}$	312 (33,700) 286 (41,200)	367 (27,450)	1.4	0.5	0.71	142
$\mathbf{L_3}$	344 (20,700) 291 (25,300)	463 (21,600)	5.5 (5.2 [17])	23 [17] , 27 [18]	0.18	0.54
$\mathbf{L_4}$	337 (34,300) 286 (33,800)	450 (22,200)	19.1	3	0.05	1.69

[a] Calculated according to $k_r = 1/\tau_{fl}$

[b] $\phi_{fl.} = k_r/(k_r + k_{nr})$

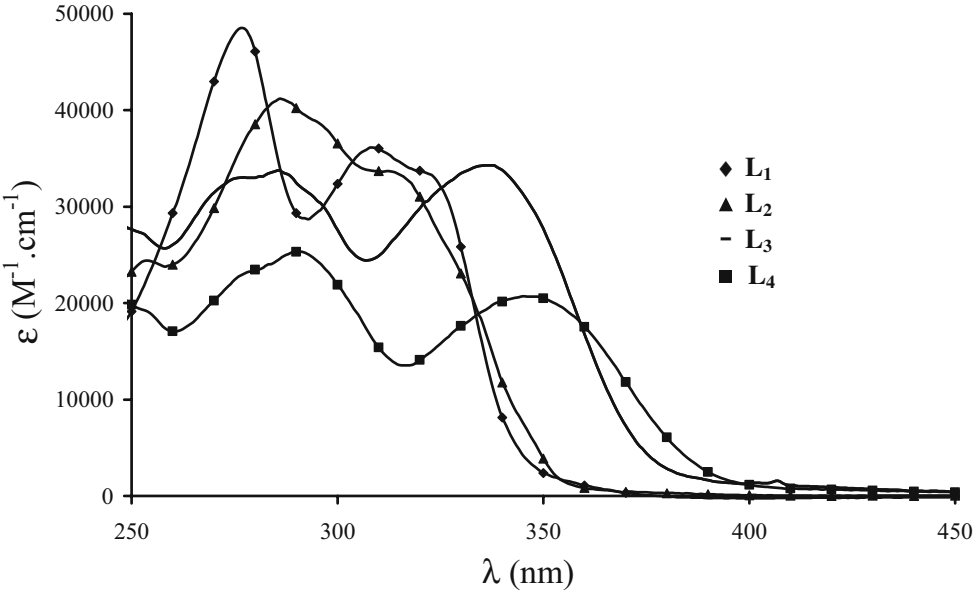

Fig. 1 UV–Vis absorption spectra of ligands $\mathbf{L_1}$ to $\mathbf{L_4}$ in CH_2Cl_2

and Fig. 1 shows their corresponding UV–Vis absorption spectra.

The absorption spectrum of $\mathbf{L_1}$ is composed of two main absorption bands attributed to $\pi \rightarrow \pi^*$ transitions centred on the tridentate unit (Fig. 1). Deprived of strong electron-donating group, $\mathbf{L_1}$ do not show any additional low energy absorption band (as observed at 387 nm for $\mathbf{L_0}$) [12]. The absorption spectrum of $\mathbf{L_2}$ is also composed of two main bands, but the energy splitting is far less pronounced, the low energy band appearing as a shoulder of the high energy tail. Comparison of $\mathbf{L_2}$ with several para-substituted phenyl terpyridines [17, 18] evidences a stabilization of the most intense absorption band observed around 278–282 nm in the reference compounds. This stabilization can also be observed in the fluorescence spectra, where the emission of $\mathbf{L_2}$ is shifted by ca. 35 nm toward lower energy compared to the references. This stabilization effect is similar to that observed with a biphenyl para-substitution [17]. Interestingly, the introduction of the vinyl spacer resulted in a large increase of the non-radiative processes with a concomitant drop of the fluorescence quantum yield compared to both the para-phenyl substituted reference compound ($\phi_{fl.}$=2%) [18] and the biphenyl one ($\phi_{fl.}$ is 2.92 times that of the para-phenyl substituted terpyridine in EtOH) [17].

The photophysical properties of $\mathbf{L_3}$ have been largely discussed in the literature [17] and will only be discussed for the understanding of the behavior of $\mathbf{L_4}$. Both $\mathbf{L_3}$ and $\mathbf{L_4}$ display similar spectra with two strong absorption bands. Molecular modelling based on density functional theory

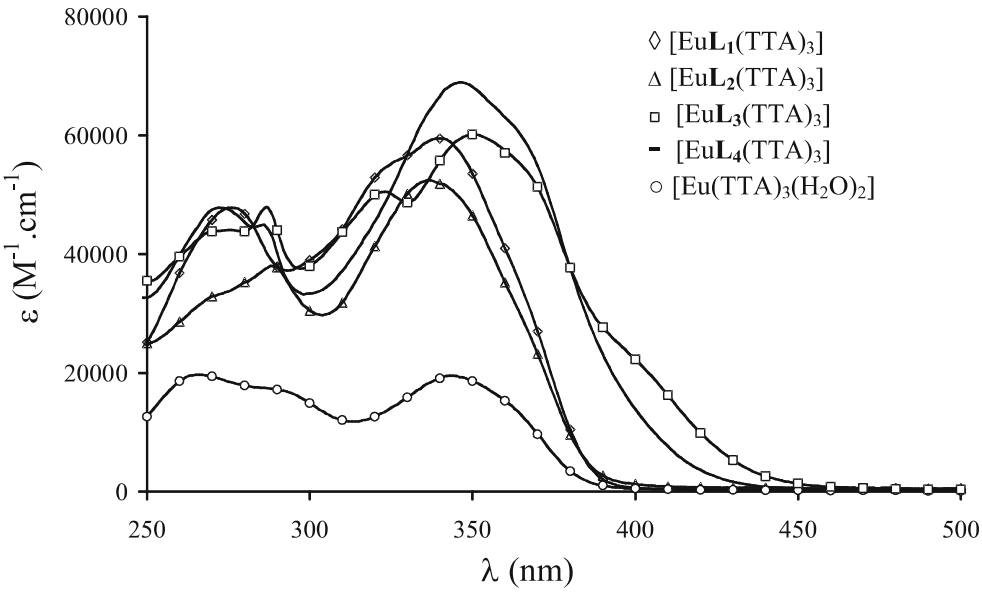

Fig. 2 UV–Vis absorption spectra of $[Eu(TTA)_3(H_2O)_2]$ and of the $[Eu\mathbf{L_n}(TTA)_3]$ complexes (n=1 to 4)

Table 2 Photophysical properties of the [Eu$\mathbf{L_n}$(TTA)$_3$] complexes in air equilibrated CH_2Cl_2 at room temperature (λ_{exc}=350 nm for all emission data)

	Absorption	Europium centred emission					
	λ_{max}/nm (ε/M^{-1} cm^{-1})	Φ_{ov} (%)	τ_{obs} (μs)	I_{MD}/I_{tot} (×100)	τ_R (μs)	Φ_{Eu} (%)	η_{sens} (%)
[Eu$\mathbf{L_1}$(TTA)$_3$]	330 (56,600)	1.4	453	9.34	2,200	21	7
[Eu$\mathbf{L_2}$(TTA)$_3$]	337 (52,400)	2.8	514	9.06	2,140	24	12
[Eu$\mathbf{L_3}$(TTA)$_3$]	345 (60,140)	20.0	555	9.39	2,210	25	80
[Eu$\mathbf{L_4}$(TTA)$_3$]	350 (68,700)	5.9	592	9.43	2,220	27	22

(DFT) calculations devoted to $\mathbf{L_3}$ and to similar para-dialkyl-aminophenyl substituted terpyridine [19] have shown that the strong electron donating substituents on the terpyridine inverted the HOMO level, which is then mainly centred on the dialkylamino moiety and gave a strong charge transfer (CT) character to the lowest energy transition. This effect is also observed with $\mathbf{L_4}$, in which the low energy transition is strongly stabilized and the absorption reaches the visible domain. A situation which is particularly attractive when lanthanide salts are chelated (*vide infra*). In all cases, the excitation spectra recorded at the emission maximum perfectly matched the corresponding absorption spectra.

The UV–Vis absorption spectra of the [Eu(TTA)$_3$(H$_2$O)$_2$] precursor [20] and of the [Eu$\mathbf{L_n}$(TTA)$_3$] complexes (n=1 to 4) in CH_2Cl_2 are presented in Fig. 2 and their main photophysical properties are gathered in Table 2.

As previously observed for the free ligands (Fig. 1), the absorption spectra of the complexes are also composed of two main absorption bands (Fig. 2). The low energy components became more intense in the complexes, due to overlapping between the absorption bands of the tridentate ligands and of the TTA moieties, as evidenced by the presence of shoulders for almost all complexes. The bathochromic shift of the low energy band is so pronounced in the complexes of $\mathbf{L_3}$ and $\mathbf{L_4}$, that the absorption reached the visible region, as observed for instance with a marked shoulder above 400 nm in [Eu$\mathbf{L_3}$(TTA)$_3$].

Upon excitation at the maximum of absorption of the low energy band, all the complexes displayed luminescence spectra revealing an admixture of ligand-centred and europium-centred luminescence in varying amounts. The former appeared as a broad nonstructured emission band in the 350–600 nm region, while the latter could be easily identified on the basis of the characteristic pattern of the $^5D_0 \rightarrow {}^7F_J$ (J=0 to 4) electronic transitions of europium around 575, 590, 615, 645 and 690–700 nm for J=0 to 4, respectively [1]. A typical example of the luminescence spectrum of [Eu$\mathbf{L_1}$(TTA)$_3$] is displayed in Fig. 3.

Interestingly, the relative contributions of ligand- or europium-centred luminescence are clearly different within the series. While the ligand-centred emission is dominant in $\mathbf{L_1}$ (Fig. 3), it becomes a minor component for complexes of $\mathbf{L_2}$ and $\mathbf{L_3}$, and is almost not observed for [Eu$\mathbf{L_4}$(TTA)$_3$] nor in the [Eu(TTA)$_3$(H$_2$O)$_2$] precursor. The question of whether the remaining ligand-centred emission was due to incom-

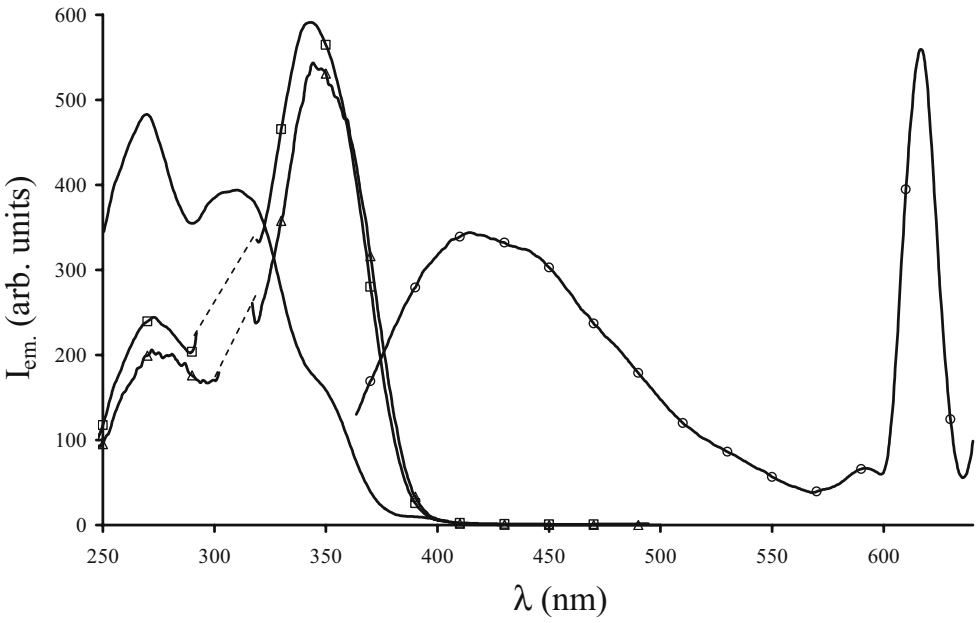

Fig. 3 Emission (λ_{exc}=350 nm, *circle*) and excitation (λ_{em}=450 nm, *full line*; λ_{em}=616 nm, *square*) spectra of [Eu$\mathbf{L_1}$(TTA)$_3$] and excitation spectra of [Eu(TTA)$_3$(H$_2$O)$_2$] (λ_{em}=616 nm, *triangle*) in CH_2Cl_2 (excitation spectra are truncated around 308 nm for 616 nm emission to remove undesired artefact originating from second order diffraction)

plete energy transfer from $\mathbf{L_1}$ to the europium or to a partial decomplexation of the tridentate ligand in diluted solutions (typically 10^{-5} M), was addressed by means of selective excitation spectra and corroborated by luminescence decay measurements of europium. In the most striking case of the [Eu$\mathbf{L_1}$(TTA)$_3$] complex, excitation spectra selectively performed at europium (λ_{em}=616 nm) or ligand (λ_{em}=450 nm) emission displayed very different patterns (Fig. 3). In the first case, the maximum of excitation rose at 344 nm. This behavior is characteristic of excitation through the TTA moieties, as evidenced by comparison with the excitation spectrum obtained with the [Eu(TTA)$_3$(H$_2$O)$_2$] precursor. In contrast, the ligand-centered emission showed the excitation to originate from higher energy transitions with a maximum at 311 nm. The europium excitation spectra of the Eu complex of $\mathbf{L_1}$ and of its TTA precursor are so similar that one can even wonder if the emission did not simply arise from the Eu(TTA)$_3$ precursor as a result of a dissociation. The answer was given by measurement of the Eu decay lifetimes at 616 nm (excitation at 350 nm), which can be correctly fitted only with a bi-exponential model, with a long lifetime of 453 μs and a short lifetime component of 260 μs, comparable to that of [Eu(TTA)$_3$(H$_2$O)$_2$] (τ= 225 μs) obtained in the same conditions. This result unambiguously points to the presence of two Eu emitting species; the Eu precursor and its $\mathbf{L_1}$ complex. From these results, it appears that the tridentate ligand $\mathbf{L_1}$ is poorly coordinated in CH_2Cl_2, leading to partial decomplexation in diluted solutions ($c<10^{-5}$ M). The data also point out a modest efficiency of the energy transfer from the tridentate ligand to the europium center. The presence of the two methyl groups on the pyrazolyl rings is probably largely responsible for such a weak coordination to the europium. This kind of steric hindrance has already been studied with bidentate ligands based on ortho- or para-substituted pyridyl rings and can have dramatic impact on the stability of the complexes and on their chemical properties [21]. Surprisingly, this dissociation in solution was not mentioned in the case of [Eu$\mathbf{L_0}$(TTA)$_3$], despite the very similar coordinating entities and the fact that it may account for the presence of the observed ligand-centred fluorescence [12].

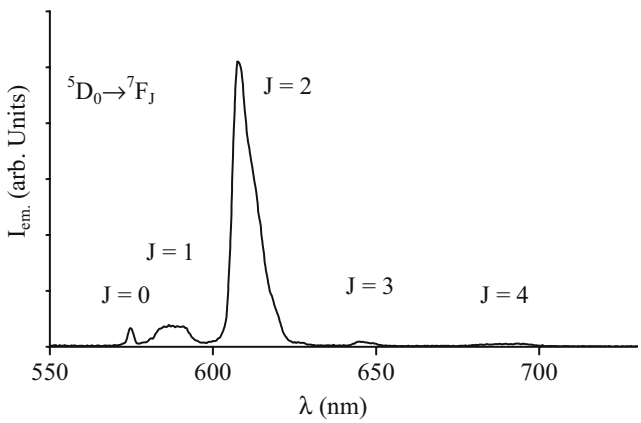

Fig. 4 Luminescence spectra of [Eu$\mathbf{L_3}$(TTA)$_3$] in CH_2Cl_2 (λ_{exc}= 350 nm, slits=0.5 nm, delay time 30 μs)

As previously mentioned, the luminescence spectra of the $\mathbf{L_2}$ to $\mathbf{L_4}$ complexes display the europium emission bands and the corresponding excitation spectra are in good agreement with the absorption spectra, pointing to excitation arising both from the $\mathbf{L_n}$ ligands and from the TTA moieties. Recording the Eu centred emission spectra at higher resolution (5 Å) after a 30 μs delay time which allows for the elimination of the residual ligand centred fluorescence signals, permitted to distinguish the different components of the ^7F_J (J=0 to 4) sublevels, as exemplified in Fig. 4 with the emission spectra of [Eu$\mathbf{L_3}$(TTA)$_3$].

It was possible to estimate the europium centred luminescence quantum yield, Φ_{Eu}, using the relationships developed by Werts et al. [22]:

$$\Phi_{Eu} = \tau_{obs}/\tau_R \quad (1)$$

$$1/\tau_R = A_{MD,0} n^3 (I_{tot}/I_{MD}) \quad (2)$$

In which τ_{obs} represents the measured luminescence lifetime and τ_R the radiative lifetime of Eu, n is the refractive index of the medium (1.425 for CH_2Cl_2), I_{tot}/I_{MD} is the measured ratio of the total area of the corrected Eu emission spectrum to the area of the $^5D_0 \rightarrow ^7F_1$ magnetic dipole allowed transition (measured from the emission spectra such as in Fig. 4) and $A_{MD,0}$ is the spontaneous emission probability of this last transition theoretically calculated to be 14.65 s^{-1}. Knowing Φ_{Eu}, the sensitization efficiency $\eta_{sens.}$, representing the efficiency of the excited ligands to populate the Eu excited level is then given by:

$$\Phi_{ov.} = \eta_{sens.} \times \Phi_{Eu} \quad (3)$$

where $\Phi_{ov.}$ represents the overall luminescence quantum yield, experimentally measured by conventional means [23] using [Ru(bipy)$_3$]Cl$_2$ in air equilibrated water (λ_{exc}=450 nm, Φ=2.8%) [24] as a reference. Measured values of $\Phi_{Ov.}$,τ_{obs} and I_{tot}/I_{MD} and calculated values of τ_R, Φ_{Eu} and $\eta_{sens.}$ for the complexes are gathered in Table 2.

The emission spectra of all complexes are very similar, resulting in similar calculated values of τ_R within the series, and pointing to very similar symmetry around the europium atom in the complexes. Interestingly, the radiative lifetimes are particularly short, as a result of the low symmetry of the complexes, loosening the symmetry rules that forbid the *f–f* electronic transitions. While the metal centred luminescence is almost the same for the three terpyridine coordinating units of $\mathbf{L_2}$ to $\mathbf{L_4}$, a smaller value was observed for the complex of $\mathbf{L_1}$, probably as a result of the equilibrium between the [Eu$\mathbf{L_1}$(TTA)$_3$] and its $\mathbf{L_1}$ free precursor (*vide*

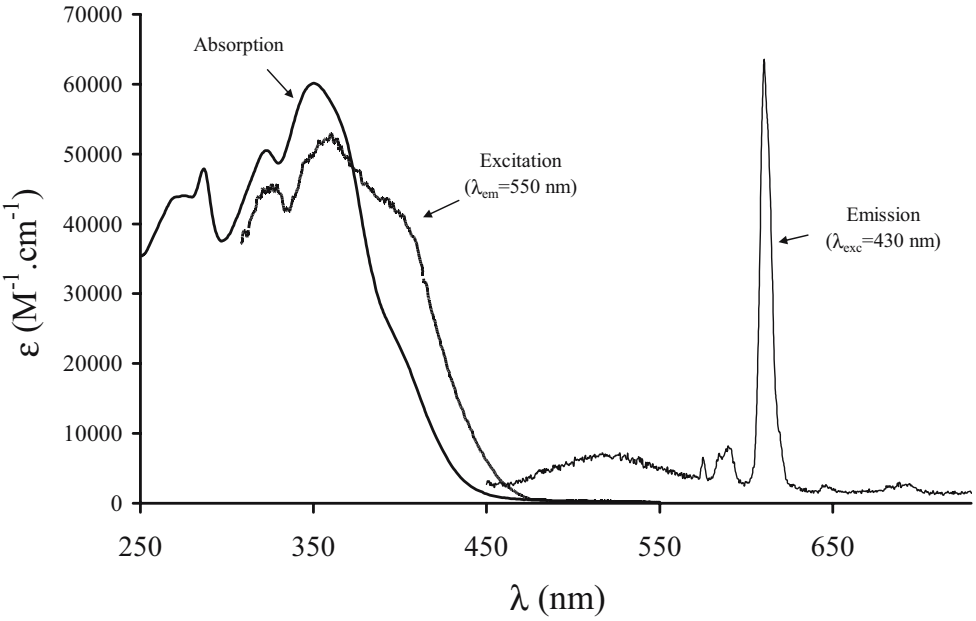

Fig. 5 Absorption, emission (λ_{exc}=430 nm) and excitation (λ_{em}=550 nm) spectra of [Eu**L**$_3$(TTA)] in CH_2Cl_2

supra). The dissociation of $\mathbf{L_1}$ freed coordination sites in the first coordination sphere of Eu, which are occupied by solvent molecules with their associated non-radiative deactivation pathways [25]. It appears that the overall luminescence quantum yields are mainly affected by the sensitization efficiencies. Interestingly, the overall trend for η_{sens} follows that of the pure ligand fluorescence efficiency (Table 1), except for $\mathbf{L_1}$, probably because of its partial decomplexation. While $\mathbf{L_1}$ and $\mathbf{L_2}$ are both poorly efficient for sensitization of the europium, $\mathbf{L_3}$ and $\mathbf{L_4}$, both enabling sensitization in the visible domain (Fig. 2), have substantial sensitization efficiencies.

While the europium complex of $\mathbf{L_3}$ presents the most important sensitization efficiency, its emission spectrum reveals the presence of a broad band with maximum at 519 nm (Fig. 5). Since the excitation was performed at 430 nm, a wavelength at which neither the free ligand nor the TTA moieties absorb, this band can be safely attributed as arising from $\mathbf{L_3}$ in the complex. This was confirmed by the corresponding excitation spectra recorded at 550 nm show-

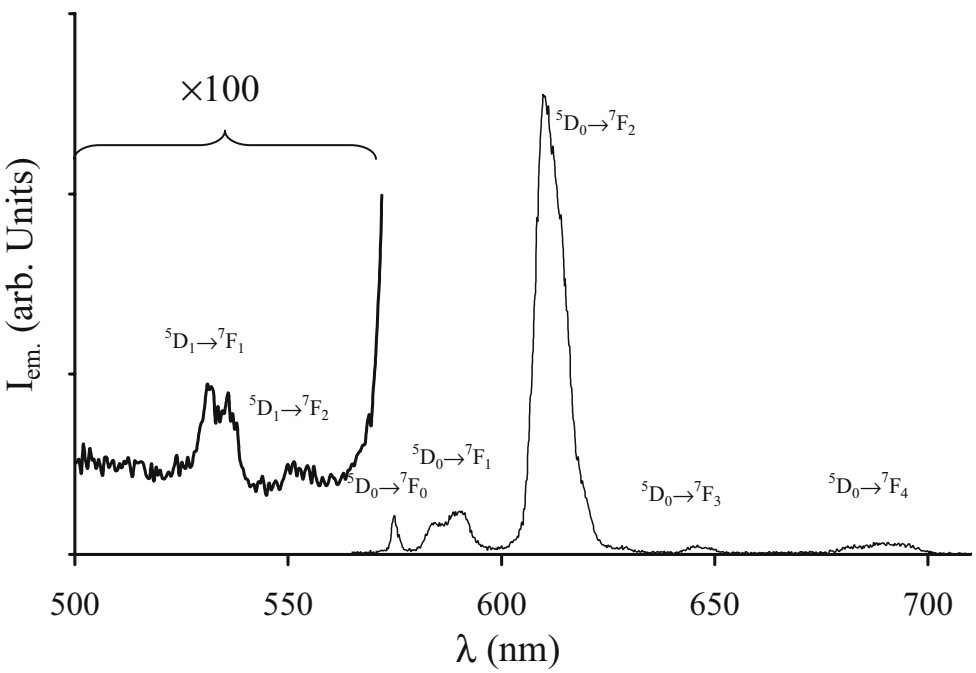

Fig. 6 Luminescence spectra of the Eu centered emission of [Eu**L**$_4$(TTA)$_3$] in CH_2Cl_2 (λ_{exc}=430 nm)

ing a strong excitation in the 400–450 nm region, at energy levels far lower than those of the free ligand or of TTA.

If the origin of the broad emission feature around 500 nm is undoubtedly ligand based, its nature could not be unambiguously attributed. In agreement with a strong solvatochromic behavior ($\lambda_{max\ em}$=457, 519 and 530 nm respectively for THF, CH_2Cl_2 and EtOH), this emission band is likely ascribed to an intra ligand charge transfer (ILCT) band localized on **L_3**. Although its short lifetime (<10 μs) suggest a singlet state, the presence of intersystem crossing processes should result in a short lived triplet state.

While the sensitization of **L_4** extends far in the visible domain, down to 430 nm, it is much less efficient for exciting the metal center. This may be attributed to the presence of efficient non-radiative pathways that exist in the free ligand itself (Table 1). Furthermore, the emission spectrum of [Eu**L_4**$(TTA)_3$] displayed a particularity within the series as it contains emission bands around 530 and 555 nm arising from the $^5D_1 \rightarrow {}^7F_{1,2}$ electronic transitions (Fig. 6), originating from direct excitation of the Eu $^5D_1$ level [26].

Conclusion

The series of tridentate N3 ligands demonstrates remarkable differences for both the coordination abilities and the photophysical properties. The results show the terpyridine moieties to be a better coordinating units than the bis (methyl–pyrazolyl)triazine, in which the presence of the methyl groups induces steric constraints resulting in partial decomplexation of the ligand in diluted solution. All the europium complexes display sizable europium centred luminescence, but the presence of a strong electron donating substitution in para position of the central chelating ring drastically improves the lanthanide luminescence. Medium resolution emission spectroscopy (5 Å) reveals very similar shapes for all spectra, in accordance with similar coordination environment around the europium atom. Applying the theoretical treatment of Werts et al. [22] resulted in similar europium radiative lifetimes and indicated that the overall luminescence efficiency is mainly governed by the sensitization efficiency. The amino functions of **L_3** and **L_4** have various effects. They first resulted in the presence of an intense absorption band with pronounced charge transfer character at lower energy. Coordination to europium further increases the electron withdrawing ability of the central pyridine ring with a concomitant bathochromic shift of the charge transfer band spanning to the visible region. Sensitization of europium complexes in the visible is of particular interest for practical applications such as labeling and biological analysis [27]. It would allow for the use of europium in time-resolved applications, without the drawbacks of UV excitation, such as the need for specific optics or pulsed UV sources. Second, the electron donating amino moiety may increase the electronic density on the pyridyl coordinating ring affording an improved coordinating strength.

For the use of such labels in bioanalytical applications, it remains to be demonstrated that a sensitization down to ca. 500 nm can still be observed in polar solvents such as water. The impacts of solvent polarity or viscosity [28] are important parameters especially when charge transfer electronic transitions are involved. Finally, such complexes may be of interest for the study of their second-order non linear optical properties [19].

Experimental section

Materials and methods ^1H and $^{13}C\{^1H\}$ NMR spectra were recorded at room temperature on Brücker Advance 300 or AC 200 spectrometers. Shifts (δ) are reported in parts per million relative to residual protons in the solvent [29]. IR were recorded in KBr disks on a Nicolet 210 spectrometer. UV–Vis absorption spectra were recorded on Uvikon 933 (Kontron Instrument) spectrophotometer. Emission spectra were recorded using a Perkin–Elmer LS 50B spectrofluorimeter equipped with a R928 (Hamamatsu) photomultiplier. Ligand excited state lifetimes were obtained on a PTI TimeMaster spectrophotometer. Emission and excitation spectra were corrected for instrumental response and were recorded in the phosphorescence mode using a 0 μs delay time and a 10 ms integration window. Europium luminescence lifetimes and high resolution europium emission spectra (5 Å) were measured on a PTI QuantaMaster spectrofluorimeter. Luminescence quantum yields were measured using the procedure described by Haas and Stein using as standards *N,N*-dimethylaminophenylterpyridine (**L_3**) for ligands ([17, 18] average value ϕ=25%) and [$Ru(bpy)_3$]Cl_2 (Φ=0.028 in air equilibrated H_2O) [24] for Eu^{3+} complexes. Fast atom bombardment (FAB, positive mode) mass spectra were recorded with ZAB–HF–VB analytical apparatus using meta-nitrobenzyl alcohol (*m*-NBA) as matrix. Chromatographic purification were performed using 0.040–0.063 mm silica gel (Merck). Thin layer chromatography (TLC) was performed on silica gel plates (Merck) coated with fluorescence indicator.

Synthesis of **2** In a Schlenk tube under argon containing anhydrous THF (5 ml) and 1-ethynyl-4-methylbenzene **1** (1.64 ml, 12.9 mmol), was added ethylmagnesium bromide (1 M in THF, 12.9 ml, 12.9 mmol). The mixture was heated at 60 °C for 2 h. The solution was cooled to 0 °C and transferred dropwise to a solution of cyanuric chloride (2.40 g, 12.9 mmol) in dry THF (5 ml) at 0 °C. The reaction mixture was stirred at 0 °C for 2 h and at r.t. overnight. The solution

was concentrated under vacuum, the resulting precipitate was dissolved in CH_2Cl_2 and purified by column chromatography over silica gel (petroleum-ether/CH_2Cl_2, 70:30 as eluent) to obtain **2** (1.81 g, 53%) as a yellow solid. ^{1}H NMR ($CDCl_3$, 300 MHz): δ 2.42 (s, 3 H), 7.24 (d, J=7.9 Hz, 2 H), 7.60 (d, J=8.1 Hz, 2 H). $^{13}C\{^1H\}$ NMR ($CDCl_3$, 75.47 MHz): δ 21.9 (CH_3), 85.7 (C≡C), 98.4 (C≡C), 116.3 (Cq), 129.6 (CH), 133.6 (CH), 142.7 (Cq), 155.5 (Cq), 171.8 (Cq). IR (cm^{-1}, KBr): 2,918 ν(CHaro), 2,222 ($\nu_{c\equiv c}$), 1,521, 1,469 ($\nu_{c\equiv c}$, C=N), 1,264, 1,255, 818 ν(C–Cl). FAB–MS m/z: 271.1 ([**2**+Li]$^+$, 100%), 273.1 ([**2**+Li]$^+$, 60%). Analytical calculation for $C_{12}H_7Cl_2N_3$: C, 54.57; H, 2.67; N, 15.91. Found: C, 54.32; H, 2.44; N, 15.73%.

Synthesis of L_1 Compound **2** (0.30 g, 1.14 mmol) was mixed with 3-methylpyrazole (0.25 ml, 3.08 mmol) and K_2CO_3 (0.39 g, 2.8 mmol) in dry acetonitrile (10 ml). The mixture was heated at 40 °C during 3 h. The solution was filtered and evaporated. The residue was dissolved in CH_2Cl_2 and purified by column chromatography over silica gel (CH_2Cl_2 100% to CH_2Cl_2/MeOH, 99.9:0.1 as eluent) to obtain compound $\mathbf{L_1}$ (0.36 g, 89%) as a slightly yellow solid. ^{1}H NMR ($CDCl_3$, 300 MHz): δ 2.31 (s, 3 H), 2.37 (s, 6 H), 6.30 (d, J=2.9 Hz, 2 H), 7.13 (d, J=7.9 Hz, 2 H), 7.54 (d, J=8.1 Hz, 2 H), 8.52 (d, J=2.6 Hz, 2 H). $^{13}C\{^1H\}$ NMR ($CDCl_3$, 75.47 MHz): δ 14.2 (CH_3), 21.7 (CH_3), 87.1 (C≡C), 94.3 (C≡C), 110.9 (CH), 117.3 (Cq), 129.3 (CH), 131.0 (CH), 133.1 (CH), 141.4 (Cq), 155.8 (Cq), 162.0 (Cq), 163.0 (Cq). IR (cm^{-1} KBr): 3,131, 2,919, 2,853 ν(CHaro), 2,211 ($\nu_{c\equiv c}$), 1,556, 1,525, 1,495, 1,431, 1,365. FAB–MS m/z: 356.3 ([$\mathbf{L_1}$ + H]$^+$, 100%). Analytical calculation for $C_{20}H_{17}N_7$: C, 67.59; H, 4.82; N, 27.59. Found: C, 67.40; H, 4.61; N, 27.21%.

Synthesis of **5** In a Schlenck tube were dissolved trans-cinnamaldehyde **4** (2.86 ml, 22.7 mmol), NaOH (0.952 g, 23.8 mmol) in a mixture of methanol (15 ml) and water (2 ml). To this colorless solution cooled at 0 °C was added 2-acetylpyridine **3** (2.67 ml, 23.8 mmol). The reaction mixture turned yellow and a yellow precipitate appeared after 15 min of stirring. The solution was stirred at 0 °C for 2 h. The solid was filtered off, washed with methanol, dissolved in CH_2Cl_2 and washed with water. The aqueous layer was extracted with CH_2Cl_2 (3×30 ml), the combined organic layers were treated with brine, dried over $MgSO_4$, filtered, and vacuum dried to give compound **5** (2.75 g, 52%) as a yellow solid. ^{1}H NMR ($CDCl_3$, 300 MHz): δ 7.00–7.18 (m, 2H), 7.27–7.46 (m, 6H), 7.64–7.78 (m, 2H), 7.85 (t, 1H, J= 7.6 Hz), 8.15 (d, 1H, J=7.6 Hz)), 8.72 (d, br, 1H, J= 4.8 Hz)). $^{13}C\{^1H\}$ NMR ($CDCl_3$, 75.47 MHz): δ 122.8 (CH), 124.6 (CH), 126.8 (CH), 127.3 (CH), 127.5 (CH), 128.9 (CH), 129.2 (CH), 136.2 (Cq), 137.0 (CH), 142.1 (CH), 144.8 (CH), 148.8 (CH), 154.3 (Cq), 189.5 (Cq). IR (cm^{-1} KBr): 2,915 ν(CHaro), 1,659 ($\nu_{C=O}$), 1,595, 1,586, 1,574 ($\nu_{c\equiv c}$), 1,347. FAB–MS m/z: 236.2 ([**5**+H]$^+$, 100%). Analytical calculation for $C_{16}H_{13}NO$: C, 81.68; H, 5.57; N, 5.95. Found: C, 81.44; H, 5.18; N, 5.58%.

Synthesis of 4'-(phenylvinyl)-2,2'/6',2"-terpyridine, L_2 1-(-2-pyridinylcarbonyl) pyridinium iodide (1.39 g, 4.25 mmol) was mixed with compound **5** (1 g, 4.25 mmol) and ammonium acetate (3.28 g, 42.5 mmol) in methanol (30 ml) under argon. The solution was heated at 65 °C during 4 h. The mixture was concentrated, the residue was dissolved in CH_2Cl_2, and washed with water. The aqueous layer was extracted with CH_2Cl_2 (3×50 ml). The combined organic layers were washed with water (50 ml), brine, dried over Na_2SO_4, filtered, and vacuum dried. The residue was dissolved in CH_2Cl_2, filtered over aluminum oxide and purified by column chromatography over silica gel (petroleum-ether/CH_2Cl_2, 20:80 to CH_2Cl_2/MeOH, 98:2 as eluent) to give compound $\mathbf{L_2}$ (0.40 g, 28%) as solid. ^{1}H NMR ($CDCl_3$, 300 MHz): δ 7.27 (d, 1H, J=16Hz), 7.32–7.45 (m, 5H), 7. 61 (d, 2H, J=6.8 Hz), 7.63 (d, 1H, J=16Hz), 7.92 (dt, J=7.7 Hz, J=1.7 Hz, 2H), 8.60 (s, 2H), 8.67 (d, J= 8.1 Hz, 2H), 8.76 (d, br, 2H, J=4.9Hz). $^{13}C\{^1H\}$ NMR ($CDCl_3$, 75.47 MHz): δ 118.2 (CH), 121.4 (CH), 123.8 (CH), 126.5 (CH), 127.1 (CH), 128.6 (CH), 128.9 (CH), 133.3 (CH), 136.5 (Cq), 136.9 (CH), 146.8 (Cq), 149.1 (CH), 155.8 (Cq), 156.3 (Cq). IR (cm^{-1} KBr): 3,047, 3,014, 2,919 ν(CHaro), 1,582, 1,566 ($\nu_{c\equiv c}$, C=N), 1,400. FAB–MS m/z: 336.2 ([$\mathbf{L_2}$ + H]$^+$, 100%). Analytical calculation for $C_{23}H_{17}N_3$: C, 82.36; H, 5.11; N, 12.53. Found: C, 82.05; H, 4.95; N, 12.45%.

Synthesis of 4'-(4-ethynyl-benzylamine)-2,2'/6',2"-terpyridine, L_4 A Schlenk flask was charged with 4-iodo-aniline (0.140 g, 0.64 mmol), 4′-ethynyl-2,2′/6′,2″-terpyridine **6** (0.111 g, 0.43 mmol) [16], $Pd(PPh_3)_4$ (0.050 g, 0.04 mmol) and *n*-propylamine (20 ml). The mixture was thoroughly degassed with argon and stirred at 60 °C for 16 h. The organic phase was filtered over celite, washed with water (150 ml) and dried over $MgSO_4$. After removal of the solvent, a chromatography on silica gel (CH_2Cl_2/MeOH, gradient from 100:00 to 99.9:0.1) afforded, after crystallization from CH_2Cl_2/cyclohexane mixture, the pure compound (0.117 g, 78%). ^{1}H NMR (d_6-DMSO, 300 MHz) δ 5.78 (s, 2H, NH_2), 6.98 (ABsys, 4H, J_{AB}=8,5 Hz, $\nu_0\delta$= 224.1 Hz), 7.52 (m, 2H), 8.02 (td, 2H, ^3J=7.8 Hz, ^4J=1.7), 8.40 (s, 2H), 8.62 (d, 2H, ^3J=8.6 Hz), 8.74 (d, 2H, ^3J= 4.0 Hz). $^{13}C\{^1H\}$ DEPT NMR (75.47 MHz, $CDCl_3$): δ 85.5 (Cq), 97.5 (Cq), 107.1 (Cq), 114.1 (CH), 121.3 (CH), 121.7 (CH), 125.1 (CH), 133.9 (CH), 134.1 (Cq), 138.0 (CH), 149.9 (CH), 151.0 (Cq), 154.9 (Cq), 155.7 (Cq). IR (KBr): 3,408, 3,318, 3,219 (νAr–NH_2), 2,919, 2,848 (νCHaro), 2,208 ($\nu_{c\equiv c}$), 1,634, 1,596, 1,581, 1,562, 1,536, 1,509, 1,468, 1,389, 1,150, 1,112, 994, 914, 873, 828 cm^{-1}. MS

(FAB+, *m*NBA): *m/z* (%)=349.5 (100) $[M+H]^+$. Analytical calculation for $C_{23}H_{16}N_4$: C, 79.29; H, 4.63; N, 16.08; Found C, 78.87; H, 4.37; N, 15.56%.

Syntheses of the complexes The lanthanide complexes were prepared according to the general procedure given for $[Eu\mathbf{L_1}(TTA)_3]$.

$[Eu\mathbf{L_1}(TTA)_3]$ To a solution of TTA–H (187 mg, 0.84 mmol) and NaOH (0.034 g, 0.85 mmol) in a mixture of methanol (15 ml) and water (2 ml) was added $EuCl_3.6H_2O$ (103 mg, 0.281 mmol). The clear solution was stirred for 10 min and a solution of $\mathbf{L_1}$ (100 mg, 0.28 mmol) in CH_2Cl_2 was added. The mixture was stirred for 30 min, after which addition of water generated a precipitate, which was filtered off and vacuum dried, affording $[Eu\mathbf{L_1}(TTA)_3]$ as a pale yellow solid (260 mg, 79%). IR (cm^{-1} KBr): 2,214 ($\nu_{c\equiv c}$), 1,602 ($\nu_{C=O}$), 1,411 (ν_{C-F}). FAB^+–$MS: m/z = 1171.2$ $\left(\left[EuL_1(TTA)_3\right]+H\right]^+, 100\%\right)$. Analytical calculation for $C_{44}H_{29}EuF_9N_7O_6S_3.4CH_3OH$: C, 44.38; H, 3.49; N, 7.55. Found: C, 44.27; H, 3.93; N, 7.96%.

$[Eu\mathbf{L_2}(TTA)_3]$ Starting from $\mathbf{L_2}$ (100 mg, 0.30 mmol), NaOH (40 mg, 0.89 mmol), TTA–H (200 mg, 0.89 mmol), and $EuCl_3.6H_2O$ (110 mg, 0.30 mmol) lead to $[Eu\mathbf{L_2}(TTA)_3]$ (150 mg, 41%). IR (cm^{-1} KBr): 1,604 ($\nu_{C=O}$), 1,535 ($\nu_{C=C}$), 1,413 (ν_{C-F}). FAB^+/MS m/z: 1,150.2 ($[Eu\mathbf{L_2}(TTA)_3]$ + $H]^+$, 80%), 1,152.2 ($[Eu\mathbf{L_2}(TTA)_3]$ + $H]^+$, 100%), 1,153.2 ($[Eu\mathbf{L_2}(TTA)_3]$ + $H]^+$, 50%). Analytical calculation for $C_{47}H_{29}EuF_9N_3O_6S_3.H_2O$: C, 48.29; H, 2.67; N, 3.59. Found: C, 48.07; H, 2.41; N, 3.28%.

$[Eu\mathbf{L_3}(TTA)_3]$ Starting from $\mathbf{L_3}$ (35 mg, 0.10 mmol), NaOH (12 mg, 0.30 mmol), TTA–H (67 mg, 0.30 mmol) and Eu $(CF_3SO_3)_3$ (60 mg, 0.10 mmol) lead to $[Eu\mathbf{L_3}(TTA)_3]$ (103 mg, 88%). IR (cm^{-1} KBr): 3,091 (ν_{C-H}), 1,598 ($\nu_{C=O}$), 1,536 ($\nu_{C=C}$), 1,413 (ν_{C-F}). FAB^+/MS m/z: 1,167.2 ($[Eu\mathbf{L_3}(TTA)_3]$ + $H]^+$, 80%), 1,169.3 ($[Eu\mathbf{L_3}(TTA)_3]$ + $H]^+$, 100%). Anal. Calc. for $C_{47}H_{32}EuF_9N_4O_6S_3$: C, 48.34; H, 2.76; N, 4.80. Found: C, 48.16; H, 2.51; N, 4.61%.

$[Eu\mathbf{L_4}(TTA)_3]$ Starting from $\mathbf{L_4}$ (50 mg, 0.14 mmol), NaOH (0.02 g, 0.43 mmol), TTA–H (100 mg, 0.43 mmol), and $EuCl_3.6H_2O$ (50 mg, 0.14 mmol). Yellow solid (0.15 g, 92%). IR (cm^{-1} KBr): 2,192 ($\nu_{C\equiv C}$), 1,606 ($\nu_{C=O}$), 1,413 (ν_{C-F}). FAB–MS m/z: 1,163.2 ($[Eu\mathbf{L_4}(TTA)_3]$ + $H]^+$, 78%), 1,165.2 ($[Eu\mathbf{L_4}(TTA)_3]$ + $H]^+$, 92%), 1,166.2 ($[Eu\mathbf{L_4}(TTA)_3]$ + $H]^+$, 40%). Analytical calculation for $C_{47}H_{28}EuF_9N_4O_6S_3.CH_2Cl_2$: C, 46.17; H, 2.42; N, 4.49. Found: C, 46.21; H, 2.70; N, 4.43%.

Acknowledgment This work was supported by the French Centre National de la Recherche Scientifique and PK gratefully acknowledges Cezanne SA (Nîmes, France) for financial support.

References

1. Bünzli J-C G, Piguet C (2005) Taking advantage of luminescent lanthanide ions. Chem Soc Rev 34:1048–1077
2. Hemmila I, Mukkala V-M (2001) Time-resolution in fluorometry technologies labels, and applications in bioanalytical assays. Crit Rev Clin Lab Sci 38:441–519
3. Charbonnière L, Hildebrandt N, Ziessel R et al (2006) Lanthanides to quantum dots resonance energy transfer in time-resolved fluoro-immunoassays and luminescence microscopy. J Am Chem Soc 128:12800–12809
4. Kido J, Okamoto Y (2002) Organo lanthanide complexes for electroluminescent materials. Chem Rev 102:2357–2368
5. Sabbatini N, Guardigli M, Lehn J-M (1993) Luminescent lanthanide complexes as photochemical supramolecular devices. Coord Chem Rev 123:201–228
6. Weissmann SI (1942) Intramolecular energy transfer, the fluorescence of complexes of europium. J Chem Phys 10:214–217
7. Quici S, Cavazzini M, Marzanni G et al (2005) Visible and near-infrared intense luminescence from water soluble lanthanide [Tb (III), Eu(III), Sm(III), Dy(III), Pr(III), Ho(III), Yb(III), Nd(III), Er (III)] complexes. Inorg Chem 44:529–537
8. Zhang J, Badger PD, Geib SJ, Petoud S (2005) Sensitization of near-infrared-emitting lanthanide cations in solution by tropolonate ligands. Angew Chem Int Ed 44:2508–2512
9. Latva M, Takalo H, Mukkala V-M et al (1997) Correlation between the lowest triplet state energy level of the ligand and lanthanide(III) luminescence quantum yield. J Lumin 75:149–169
10. Steemers FJ, Verboom W, Reinhoudt DN et al (1995) New sensitizer-modified calix[4]arene enabling near UV excitation of complexed luminescent lanthanide ions. J Am Chem Soc 117:9408–9414
11. Werts MHV, Duin MA, Hofstraat JH, Verhoeven JW (1999) Bathochromicity of Michlers ketone upon coordination with lanthanide(III) β–diketonates enables efficient sensitisation of Eu^{3+} for luminescence under visible light excitation. Chem Commun 1999:799–800
12. Yang C, Fu L-M, Wang Y, et al (2004) A highly luminescent europium complex showing visible light sensitized red emission: direct observation of the singlet pathway. Angew Chem Int Ed 43:5010–5013
13. Horrocks WD Jr, Bolender JP, Smith WD, Supkowski RM (1997) Photosensitized near infrared luminescence of ytterbium(III) in proteins and complexes occurs via an internal redox process. J Am Chem Soc 119:5972–5973
14. Lainé P, Bedioui F, Ochsenbein P et al (2002) A new class of functionalized terpyridyl ligands as building blocks for photosensitized supramolecular architectures. Synthesis, structural, and electronic characterizations. J Am Chem Soc 124:1364–1377
15. Krönhke F (1976) The specific synthesis of pyridines and oligopyridines. Synthesis 1976:1–24
16. Grosshenny V, Romero FM, Ziessel R (1997) Construction of preorganized polytopic ligands via palladium promoted cross-coupling reactions. J Org Chem 62:1491–1500
17. Goodall W, Wild K, Arm KJ, Williams JAG (2002) The synthesis of 4′-aryl substituted terpyridines by Suzuki crosscoupling reactions: substituent effects on ligand fluorescence. J Chem Soc Perkin Trans 2:1669–1681

18. Mutai T, Cheon J-D, Arita S, Araki K (2001) Phenyl-substituted 2,2′:6′,2″-terpyridines as a new series of fluorescent compounds, their photophysical properties and fluorescence tuning. J Chem Soc Perkin Trans 2:1045–1050
19. Sénéchal-David K, Hemeryck A, Tancrez N et al (2006) Synthesis, structural studies, theoretical calculations, and linear and nonlinear optical properties of terpyridyl lanthanide complexes: new evidence or the contribution of f electrons to the NLO activity. J Am Chem Soc 128:12243–12255
20. Melby LR, Rose NJ, Abramson E, Caris JC (1964) Synthesis and fluorescence of some trivalent lanthanide complexes. J Am Chem Soc 86:5117–5125
21. Charbonnière LJ, Williams AF, Piguet C et al (1998) Structural, magnetic, and electrochemical properties of dinuclear triple helices: comparison with their mononuclear analogues. Chem Eur J 4:485–493
22. Werts MHV, Jukes RTF, Verhoeven JW (2002) The emission spectrum and the radiative lifetime of Eu^{3+} in luminescent lanthanide complexes. Phys Chem Chem Phys 4:1542–1548
23. Haas Y, Stein G (1971) Pathways of radiative and radiationless transitions in europium(III) solutions. Role of solvents and anions. J Phys Chem 75:3668–3677
24. Nakamura K (1982) Synthesis, luminescence quantum yields, and lifetimes of trischelated ruthenium(II) mixed-ligand complexes including 3,3-dimethyl-2,2-bipyridyl. Bull Chem Soc Jpn 55: 2697–2705
25. Beeby A, Clarkson IM, Dickins RS et al (1999) Non radiative deactivation of the excited states of europium, terbium and ytterbium complexes by proximate energy-matched OH, NH and CH oscillators: an improved luminescence method for establishing solution hydration states. J Chem Soc Perkin Trans 2:493–503
26. e Silva FRG, Menezes JFS, Rocha GB, et al (2000) Emission quantum yield of europium (III) mixed complexes with thenoyltrifluoroacetonate and some aromatic ligands. J Alloys Compd 303–304:364–370
27. Weibel N, Charbonnière LJ, Guardigli M et al Engineering of highly luminescent lanthanide tags for protein labeling and time-resolved luminescence imaging. J Am Chem Soc 126:4888–4896
28. Valeur B (2002) Molecular fluorescence, principles and applications. Wiley–VCH: Weiheim, Germany
29. Gottlieb H, Kotlyar V, Nudelman A (1997) NMR chemical shifts of common organic laboratory solvents as trace impurities. J Org Chem 62:7512–7515